Hamiltonian structure of propagation equations for ultrashort optical pulses

Sh. Amiranashvili and A. Demircan

Weierstrass Institute for Applied Analysis and Stochastics, Mohrenstrasse 39, D-10117 Berlin, Germany
(Received 20 December 2009; revised manuscript received 5 May 2010; published 13 July 2010)

A Hamiltonian framework is developed for a sequence of ultrashort optical pulses propagating in a nonlinear dispersive medium. To this end a second-order nonlinear wave equation for the electric field is transformed into a first-order propagation equation for a suitably defined complex electric field. The Hamiltonian formulation is then introduced in terms of normal variables, i.e., classical complex fields referring to the quantum creation and annihilation operators. The derived z-propagated Hamiltonian accounts for forward and backward waves, arbitrary medium dispersion, and four-wave mixing processes. As a simple application we obtain integrals of motion for the pulse propagation. The integrals reflect time-averaged fluxes of energy, momentum, and photons transferred by the pulse. Furthermore, pulses in the form of stationary nonlinear waves are considered. They yield extremal values of the momentum flux for a given energy flux. Simplified propagation equations are obtained by reduction of the Hamiltonian. In particular, the complex electric field reduces to an analytic signal for the unidirectional propagation. Solutions of the full bidirectional model are numerically compared to the predictions of the simplified equation for the analytic signal and to the so-called forward Maxwell equation. The numerics is effectively tested by examining the conservation laws.

I. INTRODUCTION

The evolution of a wave packet is accurately described in terms of a complex envelope [1]. The latter results from a time-scale separation (e.g., when the pulse contains many field cycles). A slowly varying envelope approximation (SVEA) reduces then the second-order wave equation for the pulse electric field to a more simple first-order nonlinear Schrödinger equation (NSE) for the pulse envelope [2–4]. In the frequency domain, the SVEA assumes that the pulse spectrum is narrow, centered around a carrier frequency. However, situations for which the SVEA lacks precision are also quite common. For instance, we mention self-focusing [5,6], optical shocks [7], steep pulse edge [8], experiments with ultrashort pulses as optical event horizons [9], and supercontinuum (SC) generation [10]. An important example is that of a few-cycle or a subcycle optical pulse where the spectrum width is comparable to the carrier frequency [11–16]. In all such situations the NSE cannot be applied and either a full modeling of Maxwell equations should be undertaken [17–23] or new effective models for propagation of spectrally broad pulses should be introduced. These models can be developed in different directions.

First, we mention a generalized NSE in which an arbitrary dispersion profile is approximated by a higher-order Taylor expansion or, more exactly, by a polynomial fit in the frequency domain. The dispersion is then accounted for by a differential dispersion operator in the time domain [2,4]. The nonlinear term in the generalized NSE is further extended to capture an arbitrary pulse duration [8,24,25]. Furthermore, incorporation of Raman scattering [26,27], diffraction [24,28,29], and third-harmonic generation [30] have been discussed. The generalized NSE applies to pulse propagation, optical shocks, and SC generation [10,31–38]. It may reproduce the optical field behavior even beyond the validity of the SVEA. However, one should note that the dispersion profile for a very broad spectrum *a priori* cannot be captured by a polynomial expansion [39,40].

The second approach to the ultrashort optical pulses is to abandon the envelope concept and to operate directly with the pulse fields. The simplified model equations are derived assuming an unidirectional character of pulse propagation instead of SVEA. A recent review is given in Ref. [41]. In addition, we mention a short-pulse equation in which the dispersion function is expanded with respect to the inverse frequency [42,43] and a more general approach with the Laurent series [44–46]. Another important class of equations is given by the (mixed) modified Korteweg–de Vries and sine-Gordon models [47–52].

As a rule, such unidirectional propagation equations operate in the space-time domain, ignore absorption, and use a simplified medium response function. In return, the deduced models often allow for an exact treatment [53–56] or at least for an explicit solitary solution [41,57–63]. Also, many specific solutions to the generalized NSE can be found [33,64–76].

The third approach is to derive the pulse propagation model in the spectral domain [77–81]. Here, again using the unidirectional approximation, one obtains a set of the first-order ordinary differential equations for the field harmonics $E_\omega(z)$. The deduced models are more simple than the full second-order propagation equation and still allow for arbitrary dispersion and spectrum width.

In this paper, pulse propagation equations in the spectral domain are treated from the Hamiltonian point of view. By neglecting medium absorption and considering a one-dimensional (z-propagated) setting, we transform the second-order propagation equation for the electric field $E(z,t)$ into the first-order propagation equation for the complex electric field $\mathcal{E}(z,t)$. Positive- and negative-frequency components of $\mathcal{E}(z,t)$ correspond to the forward and backward waves, respectively. A Hamiltonian framework is then introduced for the derived propagation equation. To this end we define normal variables, $\mathcal{A}(z,t)$ and $\mathcal{A}^*(z,t)$. The latter are classical complex fields and refer to the quantum creation and annihilation operators.

By construction, the Hamiltonian is an integral of motion. Further integrals are yielded by continuous symmetries of the Hamiltonian. Because of the z-propagated formulation, the integrals are given by the time-averaged fluxes of the relevant physical quantities. They provide an effective tool to follow the numerical solution (e.g., for the SC generation scenarios). We also demonstrate that the stationary nonlinear waves can be characterized as constrained extrema of the momentum flux. Furthermore, reduction of the bidirectional model to a unidirectional one and further reduction to an envelope equation can be accomplished by simplifying the Hamiltonian function. The corresponding hierarchy of the first-order propagation equations is derived. Exemplary solutions of the bidirectional model are numerically compared to the predictions of the reduced equations.

II. DERIVATION

A. Basic equations

A formulation of the problem and notations are described in this section. We consider a sequence of linearly polarized electromagnetic pulses propagating along the z axis in a homogeneous dispersive nonlinear medium such that the diffraction effects are negligible. The pulse fields $\mathbf{E} = (E(z,t),0,0)$ and $\mathbf{B} = (0,B(z,t),0)$ are governed by Maxwell equations

$$\partial_z E = -\partial_t B, \quad -\frac{1}{\mu_0}\partial_z B = \partial_t(\epsilon_0 E + P), \quad (1)$$

where ϵ_0 and μ_0 are the permittivity and the permeability of free space, respectively. The induced medium polarization $\mathbf{P} = (P(z,t),0,0)$ depends on $E(z,t)$ and is determined by a sequence of nonlocal susceptibility operators $\hat{\chi}^{(i)}$ such that

$$P(E) = \epsilon_0(\hat{\chi}^{(1)}E + \hat{\chi}^{(2)}EE + \hat{\chi}^{(3)}EEE + \cdots), \quad (2)$$

where $\hat{\chi}^{(1)}$ is a linear operator, $\hat{\chi}^{(2)}$ is a bilinear one, and so on. The power expansion (2) assumes that pulses are propagating in a weakly nonlinear limit. In addition, an inverse symmetry is assumed such that $P(-E) = -P(E)$ and $\hat{\chi}^{(2)} = 0$. Equations (1) and (2) are reduced to a scalar nonlinear wave equation

$$\partial_z^2 E - \frac{1}{c^2}\partial_t^2(E + \hat{\chi}^{(1)}E + \hat{\chi}^{(3)}EEE) = 0 \quad (3)$$

in which only linear and cubic polarization terms are taken into account.

Integrating Eqs. (1) over time, one sees that the averaged electric and magnetic fields are constant along the z axis. For simplicity, we assume that the time-averaged fields vanish such that

$$\oint E(z,t)dt = 0 \quad \text{and} \quad \oint B(z,t)dt = 0, \quad (4)$$

where we use the notation

$$\oint dt = \int_{-T/2}^{+T/2} dt$$

and T is the period of the pulse sequence.

To proceed, we write the electric field in the frequency domain

$$E(z,t) = \sum_\omega E_\omega(z)e^{-i\omega t}, \quad \omega \in \frac{2\pi}{T}\mathbb{Z},$$

where

$$E_\omega(z) = \oint E(z,t)e^{i\omega t}\frac{dt}{T}, \quad E_\omega = E_{-\omega}^*,$$

and $E_{\omega=0} = 0$ in accord with Eq. (4). The linear susceptibility $\hat{\chi}^{(1)}E$ is defined by a convolution

$$(\hat{\chi}^{(1)}E)_\omega = \chi^{(1)}(\omega)E_\omega.$$

It yields the dielectric constant and the propagation parameter

$$\epsilon(\omega) = 1 + \chi^{(1)}(\omega) = \epsilon^*(-\omega),$$

$$k(\omega) = \frac{\omega}{c}\sqrt{\epsilon(\omega)} = \beta(\omega) + i\alpha(\omega) = -k^*(-\omega),$$

where $\beta(\omega)$ and $\alpha(\omega)$ are odd and even functions, respectively. Our main concern is the Hamiltonian framework; therefore, a small absorption limit is considered. In particular, we neglect $\alpha(\omega)$, assuming that an essential part of the pulse spectrum belongs to a transparency window.

The nonlinear susceptibility operator $\hat{\chi}^{(3)}$ is given by the expression

$$(\hat{\chi}^{(3)}EEE)_\omega = \sum_{\omega_1+\omega_2+\omega_3=\omega} \chi_{\omega_1\omega_2\omega_3\omega}^{(3)}E_{\omega_1}E_{\omega_2}E_{\omega_3}$$

in which summation is performed over suitable (resonance) triads $\{\omega_1,\omega_2,\omega_3\}$. Whenever possible, we abbreviate the sum in the last equation as

$$(\hat{\chi}^{(3)}EEE)_\omega = \sum_{123|\omega} \chi_{123\omega}^{(3)}E_{\omega_1}E_{\omega_2}E_{\omega_3}.$$

The condition $\omega_1 - \omega_2 + \omega_3 = \omega$ will be indicated as $1\bar{2}3|\omega$. In this way, summations over quads of frequencies can also be abbreviated. For instance, we will replace $\sum_{\omega_1-\omega_2+\omega_3-\omega_4=0} \chi_{\omega_1\omega_2\omega_3\omega_4}^{(3)}$ by $\sum_{1\bar{2}3\bar{4}|} \chi_{1234}^{(3)}$.

If the dispersion of $\hat{\chi}^{(3)}$ can be ignored, one is left with the cubic Kerr medium in which

$$(\hat{\chi}^{(3)}EEE)_{\text{Kerr}} = \chi E^3, \quad \chi = \text{const}. \quad (5)$$

However, for a spectrally broad pulse such an approximation may be invalid and a more general model should be used. For instance, considering a classical nonlinear oscillator model for electrons, one obtains (Miller's rule, see Ref. [4])

$$\chi_{123\omega}^{(3)} = \text{const} \times \chi^{(1)}(\omega_1)\chi^{(1)}(\omega_2)\chi^{(1)}(\omega_3)\chi^{(1)}(\omega).$$

In the following we deal with a general nonlinear susceptibility $\chi_{123\omega}^{(3)}$ only assuming that it is symmetric with respect to all permutations of frequencies as suggested by Miller's rule. The nonlinear absorption is ignored, i.e., $\chi_{123\omega}^{(3)}$ is a real and even function of frequencies. The Kerr model (5) is used as an illustration.

To proceed, we write the nonlinear wave equation (3) in the frequency domain

$$\partial_z^2 E_\omega + \beta^2(\omega)E_\omega + \frac{\omega^2}{c^2}\sum_{123|\omega} \chi_{123\omega}^{(3)}E_{\omega_1}E_{\omega_2}E_{\omega_3} = 0. \quad (6)$$

Equation (6) is the starting point of our considerations.

B. Complex field

In this section we transform Eq. (6) into a first-order propagation equation. To this end, we introduce a complex electric field

$$\mathcal{E}(z,t) = \sum_\omega \mathcal{E}_\omega(z) e^{-i\omega t},$$

where $\mathcal{E}(z,t) \in \mathbb{C}$ and therefore in general $\mathcal{E}_\omega$ differs from $\mathcal{E}^*_{-\omega} = (\mathcal{E}_{-\omega})^* = (\mathcal{E}^*)_\omega$. The notation

$$\breve{\mathcal{E}}_\omega = \frac{\mathcal{E}_\omega + \mathcal{E}^*_{-\omega}}{2} = \frac{\mathcal{E}_\omega + (\mathcal{E}^*)_\omega}{2} \qquad (7)$$

is used to separate the real part of $\mathcal{E}(z,t)$. The complex electric field is defined as a single complex counterpart of two directional variables used in Ref. [81]

$$\mathcal{E}_\omega(z) = E_\omega(z) + \frac{\omega B_\omega(z)}{|\beta(\omega)|} = E_\omega(z) - \frac{i \partial_z E_\omega(z)}{|\beta(\omega)|}, \qquad (8)$$

where the second representation is obtained from the first equation in (1). Equations (7) and (8) imply

$$\breve{\mathcal{E}}_\omega(z) = E_\omega(z), \quad E(z,t) = \frac{1}{2}\mathcal{E}(z,t) + \text{c.c.}, \qquad (9)$$

such that $\mathcal{E}(z,t)$ is a complexification of $E(z,t)$.

To get a better insight into Eq. (8), we consider, for a moment, only a linear medium. For a linear forward (backward) wave we have

$$E_\omega(z) \sim e^{\pm i\beta(\omega)z} \quad \Rightarrow \quad \mathcal{E}_\omega = \left(1 \pm \frac{\omega}{|\omega|}\right) E_\omega. \qquad (10)$$

Therefore $\mathcal{E}_{\omega>0}$ and $\mathcal{E}_{\omega<0}$ are responsible for the forward and backward waves, respectively. In particular, contributions of these waves are explicitly split in the relation $E_\omega = \frac{1}{2}(\mathcal{E}_\omega + \mathcal{E}^*_{-\omega})$.

Returning to the nonlinear case and applying an identity

$$(\partial_z^2 + \beta^2)E_\omega = (|\beta| + i\partial_z)(|\beta| - i\partial_z)E_\omega = (|\beta| + i\partial_z)|\beta|\mathcal{E}_\omega,$$

we transform Eq. (6) into the following propagation equation:

$$i\partial_z \mathcal{E}_\omega + |\beta|\mathcal{E}_\omega + \frac{\omega^2}{c^2|\beta|} \sum_{123|\omega} \chi^{(3)}_{123\omega} \breve{\mathcal{E}}_{\omega_1} \breve{\mathcal{E}}_{\omega_2} \breve{\mathcal{E}}_{\omega_3} = 0. \quad (11)$$

Equation (11) for $\mathcal{E}_\omega(z)$ is of first order. It looks similar to the unidirectional equation for $E_\omega(z)$ derived in Ref. [77],

$$i\partial_z E_\omega + \beta E_\omega + \frac{\omega^2}{2c^2\beta} \sum_{123|\omega} \chi^{(3)}_{123\omega} E_{\omega_1} E_{\omega_2} E_{\omega_3} = 0, \quad (12)$$

and can be solved using the same numerical approach. Equation (11) is, however, *exact* in the sense the unidirectional approximation was not applied. Both forward and backward waves exactly fulfill the same first-order propagation model (11) as long as the nonlinearity is calculated from the total field (9) (see also Refs. [78,79]).

C. Hamiltonian framework

A standard way to obtain first-order Hamiltonian equations is to perform a Legendre transformation of a second-order Lagrangian equation [82]. This procedure is discussed in Ref. [83] for the second-order nonlinear wave equation and

the t-propagated picture. It leads to a complicated multivalued expression for the canonical momentum. The z-propagated picture is more simple to deal with because Eq. (11) is already of first order.

In this section we introduce a Hamiltonian framework by writing Eq. (11) in terms of normal variables. To this end, we change from $\mathcal{E}(z,t)$ to a new complex field

$$\mathcal{A}(z,t) = \sum_\omega \mathcal{A}_\omega(z) e^{-i\omega t}, \quad \mathcal{E}_\omega = \sqrt{\frac{2\mu_0\omega^2}{|\beta(\omega)|}} \mathcal{A}_\omega, \quad (13)$$

define

$$T_{\omega_1\omega_2\omega_3\omega_4} = \frac{\mu_0|\omega_1\omega_2\omega_3\omega_4|\chi^{(3)}_{\omega_1\omega_2\omega_3\omega_4}}{c^2\sqrt{|\beta(\omega_1)\beta(\omega_2)\beta(\omega_3)\beta(\omega_4)|}}, \qquad (14)$$

and transform Eq. (11) into

$$i\partial_z \mathcal{A}_\omega + |\beta|\mathcal{A}_\omega + 2\sum_{123|\omega} T_{123\omega} \breve{\mathcal{A}}_{\omega_1} \breve{\mathcal{A}}_{\omega_2} \breve{\mathcal{A}}_{\omega_3} = 0, \quad (15)$$

where similar to Eq. (7)

$$\breve{\mathcal{A}}_\omega = \frac{\mathcal{A}_\omega + \mathcal{A}^*_{-\omega}}{2} \qquad (16)$$

splits contributions of the forward and backward waves. Equation (14) indicates that T_{1234} and $\chi^{(3)}_{1234}$ have the same symmetries with respect to permutations of indices.

Due to its simple and symmetric structure, Eq. (15) can be easily transformed into a Hamiltonian form

$$i\partial_z \mathcal{A}_\omega + \frac{\delta}{\delta \mathcal{A}^*_\omega} \mathsf{H} = 0 \qquad (17)$$

by defining the following Hamiltonian:

$$\mathsf{H} = \sum_\omega |\beta(\omega)||\mathcal{A}_\omega|^2 + \sum_{1234|} T_{1234} \breve{\mathcal{A}}_{\omega_1} \breve{\mathcal{A}}_{\omega_2} \breve{\mathcal{A}}_{\omega_3} \breve{\mathcal{A}}_{\omega_4}. \qquad (18)$$

Equation (17) is a complex representation of the canonical Hamiltonian equations. The classical fields $\mathcal{A}(z,t)$ and $\mathcal{A}^*(z,t)$ are complex canonical variables and refer to the creation and annihilation operators (see, e.g., Ref. [84]). By using Eq. (16) and symmetries of T_{1234}, one can transform Eq. (18) into the form

$$\mathsf{H} = \sum_\omega |\beta(\omega)|\mathcal{A}_\omega \mathcal{A}^*_\omega + \mathsf{H}_{40} + \mathsf{H}_{31} + \mathsf{H}_{22}, \qquad (19)$$

where contributions of all the possible four-wave-mixing (FWM) processes are explicitly distinguished in the last three terms,

$$\mathsf{H}_{40} = \frac{1}{16} \sum_{1234|} T_{1234}(\mathcal{A}_{\omega_1}\mathcal{A}_{\omega_2}\mathcal{A}_{\omega_3}\mathcal{A}_{\omega_4} + \text{c.c.}),$$

$$\mathsf{H}_{31} = \frac{1}{4} \sum_{123\bar{4}|} T_{1234}(\mathcal{A}_{\omega_1}\mathcal{A}_{\omega_2}\mathcal{A}_{\omega_3}\mathcal{A}^*_{\omega_4} + \text{c.c.}),$$

$$\mathsf{H}_{22} = \frac{3}{8} \sum_{1\bar{2}3\bar{4}|} T_{1234}\mathcal{A}_{\omega_1}\mathcal{A}^*_{\omega_2}\mathcal{A}_{\omega_3}\mathcal{A}^*_{\omega_4}.$$

One should stress that the system (17) and (18) is an exact reformulation of Eq. (3) in the weak absorption limit. Such a reformulation is useful for some applications which are

more difficult to address using Eq. (3). Sample applications are described in the next section.

III. APPLICATIONS

Hamiltonian formulation of a nonlinear wave equation has many important applications: integrability analysis, conservation laws, stability of solitons, and a spectrum of turbulent states to name just a few [84–86]. In this section we obtain conservation laws and relate them to the stationary nonlinear waves.

A. Momentum flux

Concerning conservation laws, special care is required when the space coordinate serves as an effective time. Consider, for instance, a standard continuity equation $\partial_t \rho + \partial_z j = 0$ for a physical quantity with the density $\rho(z,t)$ and the flux density $j(z,t)$ in one space dimension. Normally, the conserved integral is given by the "charge" $\int \rho(z,t)dz$. For the z-propagated picture we obtain $\int j(z,t)dt = \text{const}$, i.e., the time-averaged "current" is constant along the z axis.

Returning to the sequence of optical pulses, we conclude that the period average of the involved variables should not depend on the observation point z. Two simple examples are given by Eqs. (4). By construction, also the Hamiltonian (19) conserves for Eq. (17). The term $\sum_\omega |\beta(\omega)| \mathcal{A}_\omega \mathcal{A}_\omega^*$ suggests that H is related to momentum transfer. It appears that H is the period average of the momentum flux. By transforming Eq. (18) back to real fields in accord with Eqs. (8) and (13), one obtains

$$\mathsf{H} = \oint \left(\frac{\epsilon_0 \left(E + \hat{\chi}^{(1)} E + \frac{1}{2} \hat{\chi}^{(3)} EEE \right) E}{2} + \frac{B^2}{2\mu_0} \right) \frac{dt}{T}.$$

For $\hat{\chi}^{(3)} = 0$, the term in the large parentheses is a known expression for the momentum flux density in a linear medium [87]. The above expression for H is then the mean momentum flux in the nonlinear case.

B. Energy flux

Further integrals can be obtained from continuos symmetries of the Hamiltonian (19). Note, that H is invariant under the transformation $\mathcal{A}_\omega \to \mathcal{A}_\omega e^{i\omega s}$ with a free parameter s. For instance, summation in H_{40} is performed over quads of frequencies such that $\omega_1 + \omega_2 + \omega_3 + \omega_4 = 0$. Therefore, $e^{i\omega s}$ factors (appearing in $\mathcal{A}_{\omega_1} \mathcal{A}_{\omega_2} \mathcal{A}_{\omega_3} \mathcal{A}_{\omega_4}$) cancel each other. Similar arguments apply to the other terms in H.

The above continuous transformation is generated by a differential equation $i\partial_s \mathcal{A}_\omega + \omega \mathcal{A}_\omega = 0$; the latter can be transformed into a Hamiltonian equation

$$i\partial_s \mathcal{A}_\omega + \frac{\delta}{\delta \mathcal{A}_\omega^*} \sum_{\omega'} \omega' |\mathcal{A}_{\omega'}|^2 = 0.$$

Following a canonical analog of Noether's theory (see Ref. [82]), we conclude that the quantity

$$\mathsf{E} = \sum_\omega \omega |\mathcal{A}_\omega|^2 \qquad (20)$$

is an additional integral of motion for the model (17). This integral is related to energy transfer. It appears that E is the period-averaged energy flux. Returning to the real fields in Eq. (20), one obtains an averaged Poynting vector

$$\mathsf{E} = \oint \frac{EB}{\mu_0} \frac{dt}{T}.$$

Therefore, the simplest vacuum expression for the Poynting vector applies also to our nonlinear case. The sum in Eq. (20) can easily be evaluated for numerical solutions of the propagation model (15) and provides a useful tool to control numerics.

C. Stationary nonlinear waves

Stationary nonlinear waves are special solutions of propagation equations such that the wave field depends on a single variable $\tau = t - \mathfrak{b}_1 z$ (retarded time) with a free parameter $\mathfrak{b}_1$. Such solutions propagate with a constant velocity $1/\mathfrak{b}_1$ and are stationary in the comoving frame. With respect to Eq. (3), all stationary nonlinear waves can be characterized using the momentum and energy fluxes.

Let us consider H and E as functionals acting on a test function $\mathfrak{a}(\tau) = \sum_\omega \mathfrak{a}_\omega e^{-i\omega\tau}$ such that

$$\mathsf{H}[\mathfrak{a}] = \sum_\omega |\beta(\omega)| \mathfrak{a}_\omega \mathfrak{a}_\omega^* + \sum_{1234|} T_{1234} \breve{\mathfrak{a}}_{\omega_1} \breve{\mathfrak{a}}_{\omega_2} \breve{\mathfrak{a}}_{\omega_3} \breve{\mathfrak{a}}_{\omega_4},$$

$$\mathsf{E}[\mathfrak{a}] = \sum_\omega \omega \mathfrak{a}_\omega \mathfrak{a}_\omega^*, \quad \breve{\mathfrak{a}}_\omega = \frac{\mathfrak{a}_\omega + \mathfrak{a}_{-\omega}^*}{2}.$$

We now look for extremal values of $\mathsf{H}[\mathfrak{a}]$ under constrain $\mathsf{E}[\mathfrak{a}] = \text{const}$. To solve this problem, one can set the derivative of $\mathsf{H}[\mathfrak{a}] - \mathfrak{b}_1 \mathsf{E}[\mathfrak{a}]$ to zero,

$$\frac{\delta}{\delta \mathfrak{a}_\omega^*} (\mathsf{H}[\mathfrak{a}] - \mathfrak{b}_1 \mathsf{E}[\mathfrak{a}]) = \frac{\delta}{\delta \mathfrak{a}_\omega^*} \mathsf{H}[\mathfrak{a}] - \mathfrak{b}_1 \omega \mathfrak{a}_\omega = 0, \quad (21)$$

where $\mathfrak{b}_1$ is an unknown Lagrange multiplier.

The constrained problem yields both $\mathfrak{a}(\tau)$ and $\mathfrak{b}_1$. After the solution is found, one can construct

$$\mathcal{A}(z,t) = \mathfrak{a}(t - \mathfrak{b}_1 z) \quad \text{and} \quad \mathcal{A}_\omega(z) = \mathfrak{a}_\omega e^{i\mathfrak{b}_1 \omega z}.$$

Now, the latter expression for $\mathcal{A}_\omega(z)$ solves Eq. (15) because by inserting $\mathfrak{a}_\omega e^{i\mathfrak{b}_1 \omega z}$ into the equivalent Eq. (17) one obtains the extremum condition (21). Therefore, for a given energy flux, a stationary nonlinear wave yields an extremal value of the momentum flux. Furthermore, unstable nonlinear waves correspond to saddle points (see Ref. [88]).

D. Classical flux of photons

An additional integral of motion appears if contributions of both $4 \rightleftarrows 0$ and $3 \rightleftarrows 1$ four-wave processes in the Hamiltonian (19) can be neglected (or, strictly speaking, eliminated using a suitable canonical change of variables as in Ref. [84]). In that case, the Hamiltonian reduces to the form

$$\mathsf{H} = \sum_\omega |\beta| |\mathcal{A}_\omega|^2 + \frac{3}{8} \sum_{1\bar{2}3\bar{4}|} T_{1234} \mathcal{A}_{\omega_1} \mathcal{A}_{\omega_2}^* \mathcal{A}_{\omega_3} \mathcal{A}_{\omega_4}^*, \quad (22)$$

and the governing Eq. (17) becomes

$$i\partial_z \mathcal{A}_\omega + |\beta|\mathcal{A}_\omega + \frac{3}{4}\sum_{1\bar{2}3|\omega} T_{123\omega}\mathcal{A}_{\omega_1}\mathcal{A}_{\omega_2}^*\mathcal{A}_{\omega_3} = 0. \quad (23)$$

The reduced Hamiltonian (22) is invariant under an arbitrary phase shift $\mathcal{A}_\omega \to \mathcal{A}_\omega e^{i\theta}$ with a free parameter θ. This continuous transformation is generated by a differential equation $i\partial_\theta \mathcal{A}_\omega + \mathcal{A}_\omega = 0$; the latter can be transformed into a Hamiltonian equation

$$i\partial_\theta \mathcal{A}_\omega + \frac{\delta}{\delta \mathcal{A}_\omega^*}\sum_{\omega'} |\mathcal{A}_{\omega'}|^2 = 0.$$

Therefore the quantity

$$\mathsf{N} = \sum_\omega |\mathcal{A}_\omega|^2 \qquad (24)$$

is an integral of motion for the simplified pulse propagation equation (23). By analogy with quantum mechanics, N is proportional to a flux of photons. By transforming Eq. (24) back to real fields in accord with Eqs. (8) and (13), one obtains an expression for the period average of the classical photon flux

$$\mathsf{N} = \sum_\omega \frac{1}{|\beta(\omega)|}\left(\frac{\epsilon_0 \epsilon(\omega) E_\omega E_\omega^*}{2} + \frac{B_\omega B_\omega^*}{2\mu_0}\right).$$

Note, that N is infinite when conditions (4) are violated. If it is not the case, Eq. (24) provides a further useful tool to control numerics for Eq. (23).

IV. PROPAGATION EQUATIONS

In this section we describe how common unidirectional and envelope propagation equations can be derived from the Hamiltonian function (19).

A. Unidirectional approximation

As cited in the Introduction, propagation equations for short pulses are usually derived using the unidirectional approximation instead of the SVEA. In this section we explain how the unidirectional approximation applies with respect to the Hamiltonian equation (17). In accord with Eq. (10), forward and backward waves correspond to positive- and negative-frequency components of $\mathcal{E}(z,t)$. Neglecting the backward wave, we obtain

$$\begin{aligned}\mathcal{E}_{\omega>0} &= 2E_\omega, \\ \mathcal{E}_{\omega<0} &\approx 0,\end{aligned} \quad \Rightarrow \quad \mathcal{E}(z,t) = 2\sum_{\omega>0} E_\omega(z)e^{-i\omega t}.$$

In other words, the complex $\mathcal{E}(z,t)$ becomes an analytic signal corresponding to the real $E(z,t)$. Considering Eq. (19), we see that H_{40} can be ignored because the condition $\omega_1 + \omega_2 + \omega_3 + \omega_4 = 0$ cannot be satisfied for positive frequencies. Therefore the Hamiltonian (19) can be written in the form

$$\mathsf{H} = \sum_{\omega>0} \beta(\omega)\mathcal{A}_\omega \mathcal{A}_\omega^* + \mathsf{H}_{31} + \mathsf{H}_{22}, \qquad (25)$$

where summations in H_{31} and H_{22} are now performed only over positive frequencies, because $\mathcal{A}_{\omega<0} = 0$ by construction. The propagation equation (15) takes the form

$$i\partial_z \mathcal{A}_\omega + \beta(\omega)\mathcal{A}_\omega + S_{31} + S_{22} + S_{13} = 0, \qquad (26)$$

where $\omega > 0$ and

$$S_{31} = \frac{1}{4}\sum_{123|\omega} T_{123\omega}\mathcal{A}_{\omega_1}\mathcal{A}_{\omega_2}\mathcal{A}_{\omega_3},$$

$$S_{22} = \frac{3}{4}\sum_{1\bar{2}3|\omega} T_{123\omega}\mathcal{A}_{\omega_1}\mathcal{A}_{\omega_2}^*\mathcal{A}_{\omega_3},$$

$$S_{13} = \frac{3}{4}\sum_{\bar{1}2\bar{3}|\omega} T_{123\omega}\mathcal{A}_{\omega_1}^*\mathcal{A}_{\omega_2}\mathcal{A}_{\omega_3}^*.$$

At first glance, the unidirectional first-order Eq. (26) is not simpler than the bidirectional first-order Eq. (15). However, Eq. (26) is more convenient for practical uses. To a large extent one can eliminate the fast dynamics of $\mathcal{A}_\omega(z)$ by transition to a moving frame of reference. Letting V be the velocity parameter, we introduce $\mathcal{B}_\omega(z) = \mathcal{A}_\omega(z)e^{i\omega z/V}$. It is easy to see that $\mathcal{B}_\omega(z)$ is also governed by Eq. (26) but with the Doppler-shifted propagation constant $\beta(\omega) \to \tilde{\beta}(\omega) = \beta(\omega) - \omega/V$. Dynamics in the moving frame is slow if $\tilde{\beta} \ll \beta$. This transformation is especially useful when phase and group velocities are close to each other for the frequencies of interest.

B. Simplified nonlinear response

A useful and simple propagation equation results if one can neglect both the backward waves and the $3 \rightleftarrows 1$ four-wave processes. Removing H_{31} from Eq. (25), one obtains the following Hamiltonian:

$$\mathsf{H} = \sum_{\omega>0} \beta(\omega)\mathcal{A}_\omega \mathcal{A}_\omega^* + \frac{3}{8}\sum_{1\bar{2}3\bar{4}|} T_{1234}\mathcal{A}_{\omega_1}\mathcal{A}_{\omega_2}^*\mathcal{A}_{\omega_3}\mathcal{A}_{\omega_4}^*, \quad (27)$$

and the corresponding propagation equation

$$i\partial_z \mathcal{A}_\omega + \beta(\omega)\mathcal{A}_\omega + \frac{3}{4}\sum_{1\bar{2}3|\omega} T_{123\omega}\mathcal{A}_{\omega_1}\mathcal{A}_{\omega_2}^*\mathcal{A}_{\omega_3} = 0. \quad (28)$$

Here $\omega > 0$ and both summations are performed over positive frequencies. Equations (27) and (28) are unidirectional counterparts of the bidirectional Eqs. (22) and (23), respectively.

The Hamiltonian (27) is invariant with respect to phase shifts and (in addition to H and E) the classical photon flux N is conserved. For a numerical solution, Eq. (28) can be transformed to a both moving and oscillating frame of reference. Let us assume that for the frequencies of interest the propagation constant $\beta(\omega)$ is closely approximated by a linear function $\beta(\omega) \approx \beta_0 + \beta_1(\omega - \omega_0)$, where ω_0 is a reference frequency and β_0, β_1 are fit parameters. Introducing a new variable

$$\mathcal{A}_\omega(z) = \mathcal{B}_\omega(z)e^{i[\beta_0 + \beta_1(\omega-\omega_0)]z},$$

one derives that $\mathcal{B}_\omega(z)$ is also governed by Eq. (28), but with the new propagation constant

$$\tilde{\beta}(\omega) = \beta(\omega) - \beta_0 - \beta_1(\omega - \omega_0) \ll \beta(\omega), \qquad (29)$$

such that evolution of $\mathcal{B}_\omega(z)$ is slow and more convenient for the numerical treatment.

For a spectrally narrow pulse with the carrier frequency ω_0, a natural choice is $\beta_0 = \beta(\omega_0)$ and $\beta_1 = \beta'(\omega_0)$. This observation suggests that Eq. (28) is closely related to the envelope NSE while being a nonenvelope model and allowing for arbitrary $\beta(\omega)$. The relationship is investigated in the next section.

C. Envelope equation

In this section we demonstrate that the generalized NSE is just a few approximation steps away from the unidirectional Eq. (28). To this end, we return to the complex electric field (analytic signal for the case at hand) in Eq. (28) by using definition (13)

$$i\partial_z \mathcal{E}_\omega + \beta(\omega)\mathcal{E}_\omega + \frac{3\omega}{8cn(\omega)} \sum_{1\bar{2}3|\omega} \chi_{1\bar{2}3\omega} \mathcal{E}_{\omega_1}\mathcal{E}_{\omega_2}^*\mathcal{E}_{\omega_3} = 0. \quad (30)$$

Equation (30) is subject to three conservation laws:

$$\mathsf{H} = \sum_{\omega>0} n^2(\omega)\frac{\epsilon_0|\mathcal{E}_\omega|^2}{2} + \frac{3\epsilon_0}{32}\sum_{1\bar{2}3\bar{4}|}\chi_{1\bar{2}3\bar{4}}^{(3)}\mathcal{E}_{\omega_1}\mathcal{E}_{\omega_2}^*\mathcal{E}_{\omega_3}\mathcal{E}_{\omega_4}^*,$$

$$\mathsf{E} = \sum_{\omega>0} cn(\omega)\frac{\epsilon_0|\mathcal{E}_\omega|^2}{2},$$

$$\mathsf{N} = \sum_{\omega>0} \frac{cn(\omega)}{\omega}\frac{\epsilon_0|\mathcal{E}_\omega|^2}{2},$$

expressing period-averaged fluxes of momentum, energy, and photons, respectively.

To derive NSE, we introduce an envelope $\Psi(z,t)$ for some reference frequency ω_0

$$\Psi(z,t) = \sum_\Omega \Psi_\Omega(z)e^{-i\Omega t}, \quad \Psi_\Omega(z) = \mathcal{E}_{\omega_0+\Omega}(z),$$

such that

$$\mathcal{E}(z,t) = \sum_\Omega \mathcal{E}_{\omega_0+\Omega}(z)e^{-i(\omega_0+\Omega)t} = \Psi(z,t)e^{-i\omega_0 t}.$$

The real electric field is expressed as

$$E(z,t) = \mathrm{Re}[\mathcal{E}(z,t)] = \tfrac{1}{2}\Psi(z,t)e^{-i\omega_0 t} + \mathrm{c.c.},$$

in accord with the definition of the envelope [1]. Note, that SVEA is avoided because the transformation from $\mathcal{E}(z,t)$ to $\Psi(z,t)$ is a trivial change of variables. Returning now to Eq. (30), we change to $\Psi_\Omega(z)$, approximate $\chi^{(3)}_{\omega_1\omega_2\omega_3\omega}$ by $\chi_0 = \chi^{(3)}_{\omega_0\omega_0\omega_0\omega_0}$, and obtain

$$i\partial_z\Psi_\Omega + \beta(\omega_0+\Omega)\Psi_\Omega + \frac{3(\omega_0+\Omega)\chi_0}{8cn(\omega_0+\Omega)}(|\Psi|^2\Psi)_\Omega = 0.$$

Changing to

$$\Psi_\Omega(z) = \psi_\Omega(z)e^{i(\beta_0+\beta_1\Omega)z},$$

we perform a standard transformation to a moving frame

$$\Psi(z,t) = \psi(z,\tau)e^{i\beta_0 z}, \quad \tau = t - \beta_1 z,$$
$$E(z,t) = \tfrac{1}{2}\psi(z,t-\beta_1 z)e^{i(\beta_0 z-\omega_0 t)} + \mathrm{c.c.},$$

and obtain

$$i\partial_z\psi_\Omega + \tilde{\beta}(\omega_0+\Omega)\psi_\Omega + \frac{3(\omega_0+\Omega)\chi_0}{8cn(\omega_0+\Omega)}(|\psi|^2\psi)_\Omega = 0,$$

where $\tilde{\beta}$ is defined by Eq. (29).

The resulting equation, in which $n(\omega_0+\Omega)$ is often replaced by $n(\omega_0)$, is the generalized NSE for ultrashort pulses [8,24,25]. In the reduction of Eq. (30), we only approximate the operator $\chi^{(3)}$. For instance, the NSE and the field based Eq. (30) are trivially equivalent for the Kerr medium. This illustrates why the commonly used generalized NSE reproduces ultrashort pulse propagation observed experimentally in photonic crystal fiber, far beyond the validity of the SVEA [10]. Furthermore, one immediately obtains H, E, and N in terms of the envelope.

V. SIMULATIONS OF PULSE PROPAGATION

Our first objective in this section is to present numerical solutions of the first-order propagation equation generated by the full bidirectional Hamiltonian (19). Second, we compare the bidirectional model to a simpler propagation equation generated by the Hamiltonian (27) and to the so-called forward Maxwell equation [77]. To highlight complex and comprehensive propagation dynamics, we regard intense ultrashort pulses propagating in a photonic crystal fiber to generate a SC, which is characterized by a dramatic spectral broadening. Throughout this section we neglect the dispersion of the nonlinear suceptibility $\hat{\chi}^{(3)}$ and consider instantaneous nonlinear polarization (5).

The bidirectional propagation equation corresponding to the Hamiltonian (19) is transformed into the bidirectional model for the complex field $\mathcal{E}(z,t)$ (BMCF)

$$i\partial_z\mathcal{E}_\omega + |\beta(\omega)|\mathcal{E}_\omega + \frac{\omega^2\chi}{8c^2|\beta(\omega)|}[(\mathcal{E}+\mathcal{E}^*)^3]_\omega = 0, \quad (31)$$

where the real optical electric field $E(z,t) = \mathrm{Re}[\mathcal{E}(z,t)]$. BMCF describes both the third-harmonic generation and the self-steepening effect for interacting forward and backward waves.

With reasonably given initial conditions, the solutions of the BMCF facilitate then a direct comparison with results obtained by the forward Maxwell equation (12) (FME, Refs. [77–79]), which for the case at hand reads

$$i\partial_z E_\omega + \beta(\omega)E_\omega + \frac{\omega^2\chi}{2c^2\beta(\omega)}(E^3)_\omega = 0. \quad (32)$$

A further comparison is made with the simplified forward model for the analytic signal (FMAS), corresponding to the Hamiltonian (27). For $\mathcal{E}_{\omega>0}(z)$, the FMAS reads

$$i\partial_z\mathcal{E}_\omega + \beta(\omega)\mathcal{E}_\omega + \frac{3\omega^2\chi}{8c^2\beta(\omega)}(|\mathcal{E}|^2\mathcal{E})_{\omega>0} = 0. \quad (33)$$

Here $\mathcal{E}_{\omega<0}(z) = 0$ by construction and $\mathcal{E}(z,t)$ is an analytic signal for $E(z,t)$. The field-based FMAS can be transformed into the envelope-based NSE for arbitrary pulse widths without using the SVEA.

The period-averaged momentum flux H and the period-averaged energy flux E [Eqs. (19) and (20)] are used as control parameters for the accuracy of the solutions of BMCF. The

classical photon flux N [Eq. (24)] is used as a further control parameter for FMAS. To assure conservation of E, H, and N for an equidistant mesh of time points, we need at least $\Delta t = 0.2$ fs. Depending on the initial pulse width, we have to use a resolution of 2^{14} and 2^{15} harmonics for a periodic time window $T = 3.5$ ps and $T = 7$ ps, respectively. Several test calculations were performed for a better resolution, 2^{17}. The increase of the resolution does not affect the results.

A. Numerical procedure

Here, the direct split-step Fourier approach [3] either requires very small space steps or lacks precision for a few-cycle optical pulse and relatively long (e.g., 1 cm) propagation distance, such that the integrals of motion do not conserve. For our numerics we use, therefore, a de-aliased pseudospectral method. The latter originates from the computational fluid dynamics [89] and provides a numerical implementation in an very efficient and accurate manner. The method calculates all linear operators and derivatives in the frequency domain and performs the nonlinear multiplications in the time domain, with the transformations between the domains achieved by the fast Fourier transform. The integration for the linear and nonlinear part is performed in the frequency domain by a precise Runge-Kutta integration scheme of order eight with adaptive step-size control, depending on the accuracy as described in Ref. [90].

The fiber parameters of the highly nonlinear microstructured fiber are taken from [91]. The propagation constant $\beta(\omega)$, traditionally approximated by polynomials in $\omega - \omega_0$, quickly diverges for large frequencies. Instead, we use a proper rational approximation for the refractive index as in [40], which gives a correct asymptotic of chromatic dispersion for higher frequencies and avoids unnecessary numerical stiffness. The real refractive index is then given by

$$n(\omega) = \frac{p_0 + p_1\omega + \cdots + p_5\omega^5}{1 + q_1\omega + \cdots + q_5\omega^5}$$

with the following parameters: $p_0 = 1.006\,54$, $p_1 = -2.314\,31$ fs, $p_2 = 1.959\,42$ fs^2, $p_3 = -0.678\,111$ fs^3, $p_4 = 0.120\,882$ fs^4, $p_5 = -0.009\,110\,63$ fs^5 and $q_1 = -2.299\,67$ fs, $q_2 = 1.947\,27$ fs^2, $q_3 = -0.673\,382$ fs^3, $q_4 = 0.120\,015$ fs^4, $q_5 = -0.009\,051\,04$ fs^5. The value of the nonlinear susceptibility χ can be obtained from the nonlinear refractive index n_2 by $\chi = \frac{8}{3}n(\omega_0)n_2$. For the input pulse electric field we choose

$$E(z,t)|_{z=0} = \frac{1}{2}[\Psi_0 \cosh^{-1}(t/t_0)e^{-i\omega_0 t} + \text{c.c.}],$$

having a central angular frequency ω_0 and a hyperbolic-secant shape for the initial envelope with amplitude Ψ_0 and width t_0. In the following we study the nonlinear propagation of a 50- and 10-fs pulse, injected at a central frequency $\omega_0 = 2.325\,48$ PHz, corresponding to a pump wavelength $\lambda_0 = 810$ nm in the vicinity of the zero dispersion wavelength in the anomalous dispersion regime. The input pulse amplitude, width, and the fiber parameters determine the dispersion length L_D and the nonlinear length L_{NL} such that

$$L_D^{-1} = \frac{|\beta_2|}{t_0^2} \quad \text{and} \quad L_{NL}^{-1} = \frac{\omega_0}{c}n_2\Psi_0^2,$$

where $\beta_2 = \beta''(\omega_0)$. The input soliton order N equals $(L_D/L_{NL})^{1/2}$. For our simulations we choose Ψ_0 such that $N = 3.54$ for the 50-fs pulse and $N = 2.24$ for the 10 fs pulse.

B. Backscattered optical field components

To investigate numerically the effect of backscattered components of the optical field in the case of nearly unidirectional propagation, we regard the BMCF. Forward propagation of the input pulse is justified by the initial conditions

$$[\mathcal{E}_{\omega>0}(z) = 2E_\omega(z)]_{z=0} \quad \text{and} \quad \mathcal{E}_{\omega<0}(z)|_{z=0} = 0,$$

where we neglected initial components of backward propagating waves.

Figure 1 shows the density plots in the (ω,z) plane of the spectral evolution for positive and negative frequencies for an input pulse with $t_0 = 50$ fs and $t_0 = 10$ fs, respectively. The spectra are shown on a logarithmic scale. The spectral broadening of the 50-fs pulse [Fig. 1(a)] in the range between
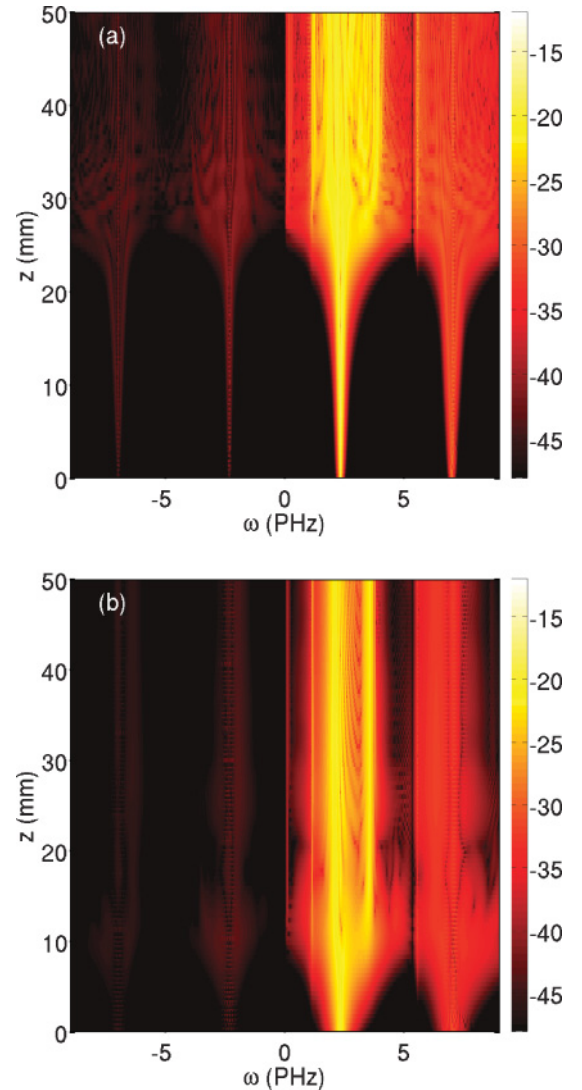

FIG. 1. (Color online) Evolution of $\chi|\mathcal{E}_\omega|^2$ in the (ω,z) plane for the 50-fs pulse (a), and the 10-fs pulse (b). The spectra are shown in logarithmic scale (dB). Negative frequencies reflect backscattered optical field components.
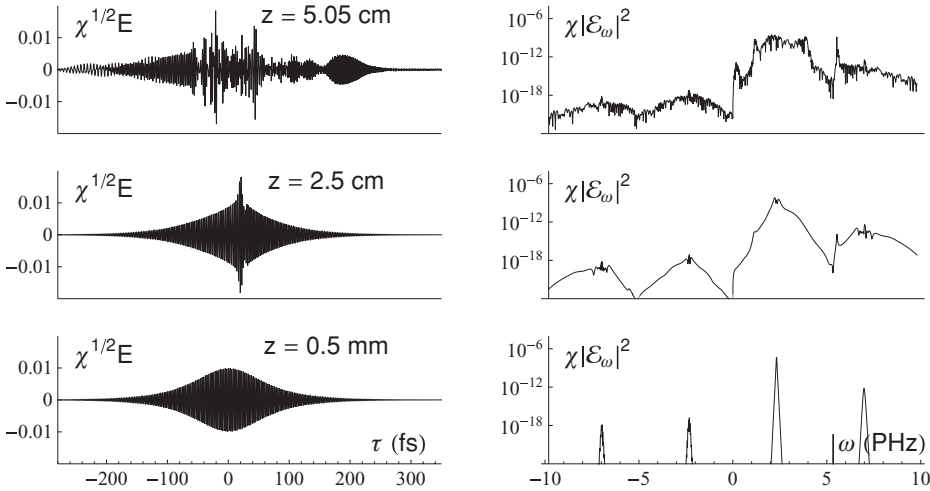
FIG. 2. Exemplary profiles of the forward propagating electric field and the corresponding spectra of the full complex field for a 50-fs pulse. The temporal profiles are shown in a forward comoving frame with $\tau = t - \beta_1 z$.

0–5 PHz exhibits the typical scenario for SC generation by soliton fission, demonstrated by modeling both the FME [77] and the generalized NSE [10]. Snapshots of the temporal shapes for selected propagation distances and corresponding spectra are presented in Fig. 2. For $\omega > 5$ PHz the spectral evolution is determined by third-harmonic generation, featuring similar broadening for the third-harmonic components. The properties of backscattered components of the optical field are represented by negative frequencies. From the beginning of the propagation the main pulse and the third harmonic lead to the excitation of two extremely weak counterparts of backward waves on the negative side of the spectrum. The strong initial contraction of the main pulse and the fission of fundamental solitons results in an enhanced spectral broadening, reflected also by the negative frequencies, which evolve in an analogous manner (see also Fig. 2 at $z = 2.5$ cm). After the breakup of the higher-order soliton (Fig. 2 at $z = 5.05$ cm) the spectral width is already saturated, but FWM generates complicated substructures, which leads to a complicated substructure for all negative frequencies.

Also for the 10-fs pulse [Fig. 1(b)], the nonlinear coupling causes a similar spectral evolution for negative frequencies as for the positive frequencies even though the input energy is reduced and the energy shift to negative frequencies is

consequently smaller. The soliton order is lower, so that SC generation by the known soliton fission process is less efficient. Snapshots of the temporal shapes for selected propagation distances and corresponding spectra are presented in Fig. 3. The strong initial spectral broadening is mainly generated by self-phase modulation and soliton compression and the spectrum reaches an octave coverage after only a few mm. In the time domain we observe one main pulse in the anomalous dispersion regime, forming one fundamental soliton, whereas the rest of the incident pulse in the normal dispersion regime disperses. After the fundamental soliton is generated, the spectrum becomes almost frozen ($z > 20$ mm). Again there is an excitation of two main components of backscattered light with negative frequencies and the spectral broadening on the negative side follows the pump pulse compression and the accompanied spectral broadening of the third harmonics. The FWM interaction of radiated dispersive waves and ejected fundamental solitons is low and the spectral profile of the backward waves retains an unruffled shape. However, the negative spectral components generated by the nonlinear coupling remain negligibly small and the propagation of the forward waves remains unaffected by their interaction.

In Fig. 4 we present the temporal evolution of the backward moving waves for the 10-fs pulse (left column) and 50-fs pulse
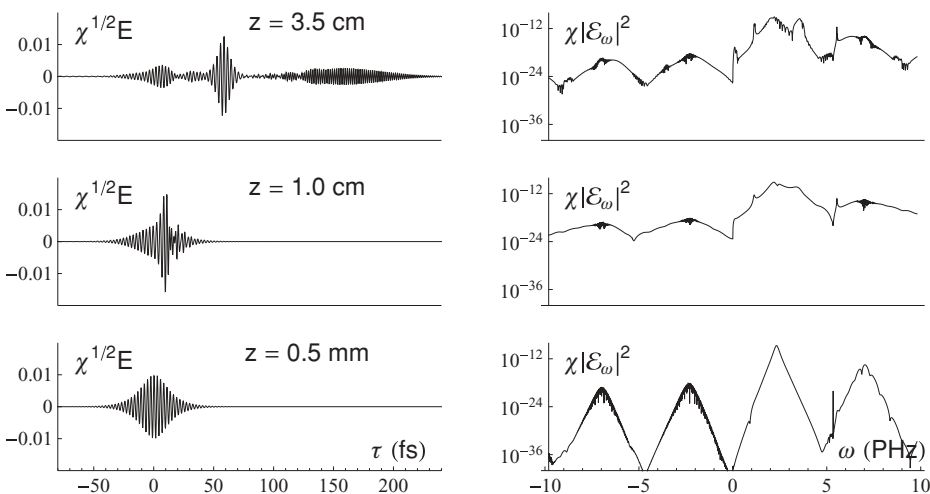

FIG. 3. Exemplary profiles of the forward propagating electric field and the corresponding spectra of the full complex field for a 10-fs pulse. The temporal profiles are shown in a forward comoving frame with $\tau = t - \beta_1 z$.
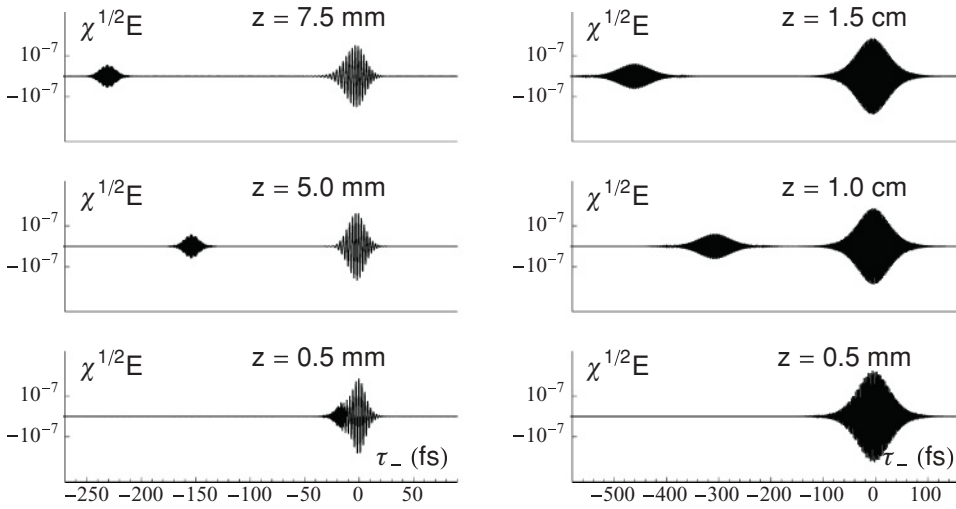
FIG. 4. Exemplary time profiles of the backscattered electric field components for a 10-fs pulse (left column) and a 50-fs pulse (right column). The profiles are shown in a backward comoving frame with $\tau_- = t + \beta_1 z$.

(right column) for selected propagation distances. The z values are chosen such that the backward waves are not superposed with the forward waves in our periodic time window and well-separated pulses can be observed. The two backward propagating field components have their center at $t = 0$ at the beginning of the propagation with the same temporal profile and width as the incident forward propagating pump wave and the third harmonics, but with amplitudes, which are several magnitudes lower. They propagate in the opposite direction with the same velocity as the forward propagating parts, so that the backscattered field components of the third harmonic move faster than the backscattered field components of the input pulse moving with the group velocity β_1^{-1}. The propagation of the backward waves is mainly affected by the linear part of BMCF and the temporal profiles stay unchanged over the regarded propagation distances.

The amplitude of the backscattered components depends on the nonlinear term in BMCF and increases with the nonlinear susceptibility χ. For the given pulse and fiber parameters the shift of energy to negative frequencies is extremely weak and the impact of backscattered light on the propagation dynamics of the forward wave can be neglected. We demonstrate this in the next section by comparing the predictions of the BMCF with simulation of the FME and the FMAS.

C. Comparison with unidirectional models

In this section we concentrate on the dynamics of the forward-propagating waves, represented by positive frequencies. The spectral evolution of the electric field components of the 10-fs pulse and the 50-fs pulse obtained by the BMCF (solid black line), the FME (solid gray line), and the FMAS (dashed black line) are presented in Fig. 5.

The solutions of the BMCF for positive frequencies do not differ globally from the solutions of the FME. The FMAS lacks $3 \rightleftarrows 1$ four-wave processes and no third-harmonic generation is observed, but in the spectral range 0–5PHz the same spectra are received as by the BMCF or the FWE. The differences between the three models are more visible in Fig. 6, where the spectra for the 50-fs pulse are shown in logarithmic and linear scale and around the carrier frequency. For the FMAS there is no energy shift to backscattered optical field components and to higher harmonic generation and the main pulse contains more energy. The SC generation evolves slightly faster in that case (dashed line). A similar deviation exists between the BMCF and the FME, whereas the energy difference lies only in shift of energy to the backward waves.

In short, predictions of all three models are very similar around the pulse carrier frequency. Therefore also the
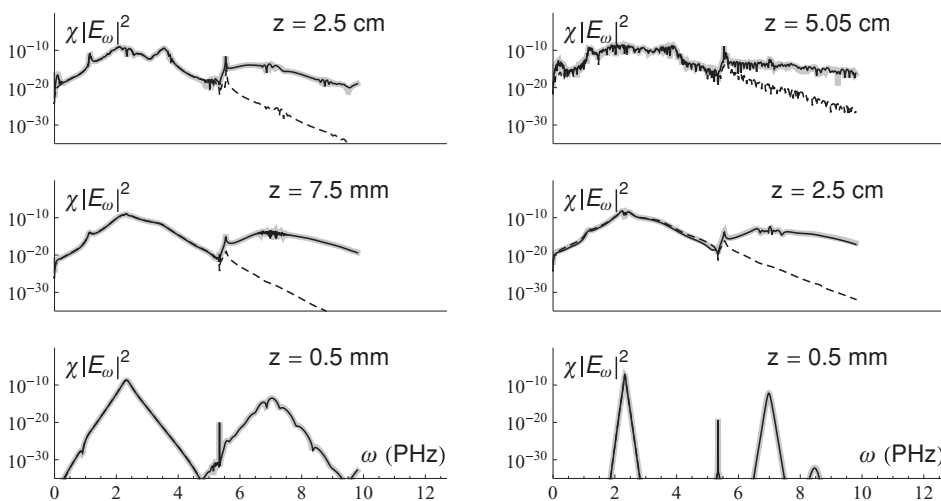

FIG. 5. Electric field spectra for selected propagation distances for a 10-fs pulse (left) and 50-fs pulse (right). Calculations were performed with the BMCF (solid black line), the FME (solid gray line), and the FMAS (dashed black line).
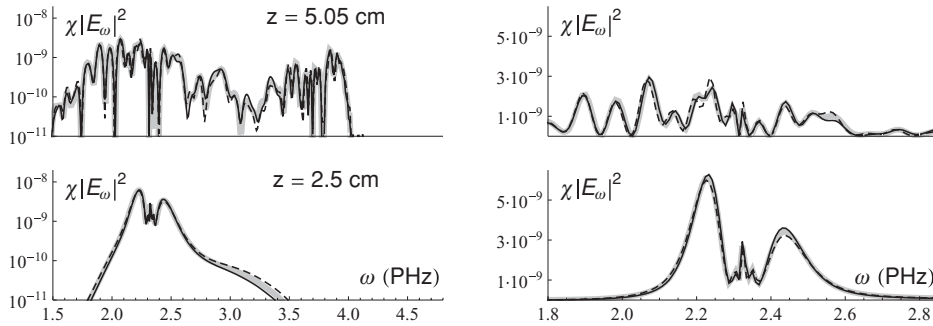
FIG. 6. Detailed comparison of the spectra predicted by the BMCF (solid black line), the FME (solid gray line), and the FMAS (dashed black line) around the carrier frequency for a 50-fs pulse in logarithmic scale (left) and linear scale (right).

simplest FMAS reproduces the most essential features of pulse propagation. Even for a relatively long propagation distance, the transfer of energy for third-harmonics generation and for a backscattered wave remains small and, most important, there is no noticeable feedback to the main pulse. The quality of all presented numerical solutions is effectively controlled by the conservation laws.

VI. CONCLUSIONS

Let us summarize our results. Propagation of spectrally broad ultrashort optical pulses is considered. First, we show how the standard second-order propagation equation can be transformed into a first-order model for a properly chosen complex electric field. The model looks similar to the first-order unidirectional models reported previously; however, it accounts for both forward and backward waves. These waves are described by positive- and negative-frequency components of the complex electric field. The latter reduces to an analytic signal for the purely forward waves.

Second, we present the bidirectional first-order propagation equation as a Hamiltonian one. To this end the so-called normal variables (classical counterparts of the creation and annihilation operators) are introduced. Then we obtain conservation laws for the z-propagated picture. They are given by the time-averaged fluxes of momentum, energy, and photons transferred by the pulse. The conservation laws provide a useful tool to control numerical solutions. They can also be used to characterize solitons. In particular, a stationary nonlinear wave is governed by the following property: the wave yields an extremal value of the momentum flux for a given energy flux. We also show that both nonenvelope (unidirectional) and envelope propagation equations can be derived directly from the Hamiltonian representation.

Finally, we illustrate numerically the propagation dynamics described by the bidirectional model for the complex field by calculating supercontinuum generation for ultrashort pulses. The solutions reproduce all essential features seen in a number of experiments [10,92] and in simulations with the generalized nonlinear Schrödinger equation [10]. In addition, the effect of backscattered optical field components can be investigated. A comparison with the forward Maxwell equation [77–79] and with the simplified equation for the analytic signal exemplifies that under certain circumstances also the latter model represents a practical and useful tool for the description of pulse propagation in nonlinear media.

[1] M. Born and E. Wolf, *Principles of Optics*, 7th ed. (Cambridge University Press, Cambridge, 1999).

[2] Y. Kodama and A. Hasegawa, IEEE J. Quantum Electron. **23**, 510 (1987).

[3] G. P. Agrawal, *Nonlinear Fiber Optics*, 4th ed. (Academic, New York, 2007).

[4] R. W. Boyd, *Nonlinear Optics*, 3rd ed. (Academic, New York, 2008).

[5] J. K. Ranka and A. L. Gaeta, Opt. Lett. **23**, 534 (1998).

[6] J. E. Rothenberg, Opt. Lett. **17**, 1340 (1992).

[7] F. DeMartini, C. H. Townes, T. K. Gustafson, and P. L. Kelley, Phys. Rev. **164**, 312 (1967).

[8] P. Kinsler and G. H. C. New, Phys. Rev. A **67**, 023813 (2003).

[9] T. G. Philbin, C. Kuklewicz, S. Robertson, S. Hill, F. Konig, and U. Leonhardt, Science **319**, 1367 (2008).

[10] J. M. Dudley, G. Genty, and S. Coen, Rev. Mod. Phys. **78**, 1135 (2006).

[11] K. Akimoto, J. Phys. Soc. Jpn. **65**, 2020 (1996).

[12] A. V. Kim, M. Y. Ryabikin, and A. M. Sergeev, Usp. Fiz. Nauk **42**, 54 (1999).

[13] T. Brabec and F. Krausz, Rev. Mod. Phys. **72**, 545 (2000).

[14] P. M. Paul, E. S. Toma, P. Breger, G. Mullot, F. Augé, P. Balcou, H. G. Muller, and P. Agostini, Science **292**, 1689 (2001).

[15] M. Hentschel, R. Kienberger, C. Spielmann, G. A. Reider, N. Milosevic, T. Brabec, P. Corkum, U. Heinzmann, M. Drescher, and F. Krausz, Nature (London) **414**, 509 (2001).

[16] M. Drescher, M. Hentschel, R. Kienberger, G. Tempea, C. Spielmann, G. A. Reider, P. B. Corkum, and F. Krausz, Science **291**, 1923 (2001).

[17] P. M. Goorjian, A. Taflove, R. M. Joseph, and S. C. Hagness, IEEE J. Quantum Electron. **28**, 2416 (1992).

[18] R. G. Flesch, A. Pushkarev, and J. V. Moloney, Phys. Rev. Lett. **76**, 2488 (1996).

[19] L. Gilles, J. V. Moloney, and L. Vázquez, Phys. Rev. E **60**, 1051 (1999).

[20] V. P. Kalosha and J. Herrmann, Phys. Rev. A **62**, 011804 (2000).

[21] J. C. A. Tyrrell, P. Kinsler, and G. H. C. New, J. Mod. Opt. **52**, 973 (2005).

[22] Y. Mizuta, M. Nagasawa, M. Ohtani, and M. Yamashita, Phys. Rev. A **72**, 063802 (2005).

[23] V. E. Semenov, JETP **102**, 34 (2006).

[24] T. Brabec and F. Krausz, Phys. Rev. Lett. **78**, 3282 (1997).

[25] P. Kinsler and G. H. C. New, Phys. Rev. A **69**, 013805 (2004).

[26] K. J. Blow and D. Wood, IEEE J. Quantum Electron. **25**, 2665 (1989).

[27] N. Karasawa, S. Nakamura, N. Nakagawa, M. Shibata, R. Morita, H. Shigekawa, and M. Yamashita, IEEE J. Quantum Electron. **37**, 398 (2001).

[28] M. A. Porras, Phys. Rev. A **60**, 5069 (1999).

[29] M. Geissler, G. Tempea, A. Scrinzi, M. Schnürer, F. Krausz, and T. Brabec, Phys. Rev. Lett. **83**, 2930 (1999).

[30] G. Genty, P. Kinsler, B. Kibler, and J. M. Dudley, Opt. Express **15**, 5382 (2007).

[31] A. A. Zozulya, S. A. Diddams, and T. S. Clement, Phys. Rev. A **58**, 3303 (1998).

[32] A. A. Zozulya, S. A. Diddams, A. G. Van Engen, and T. S. Clement, Phys. Rev. Lett. **82**, 1430 (1999).

[33] C. E. Zaspel, Phys. Rev. Lett. **82**, 723 (1999).

[34] Q.-H. Park and S. H. Han, Phys. Rev. Lett. **84**, 3732 (2000).

[35] N. Aközbek, M. Scalora, C. M. Bowden, and S. L. Chin, Opt. Commun. **191**, 353 (2001).

[36] M. S. Syrchin, A. M. Zheltikov, and M. Scalora, Phys. Rev. A **69**, 053803 (2004).

[37] A. Demircan and U. Bandelow, Opt. Commun. **244**, 181 (2005).

[38] A. Demircan and U. Bandelow, Appl. Phys. B **86**, 31 (2007).

[39] K. E. Oughstun and H. Xiao, Phys. Rev. Lett. **78**, 642 (1997).

[40] S. Amiranashvili, U. Bandelow, and A. Mielke, Opt. Commun. **283**, 480 (2010).

[41] A. I. Maimistov, Quantum Electron. **30**, 287 (2000).

[42] T. Schäfer and C. E. Wayne, Physica D **196**, 90 (2004).

[43] Y. Chung, C. K. R. T. Jones, T. Schäfer, and C. E. Wayne, Nonlinearity **18**, 1351 (2005).

[44] S. A. Kozlov and S. V. Sazonov, JETP **84**, 221 (1997).

[45] V. G. Bespalov, S. A. Kozlov, Y. A. Shpolyanskiy, and I. A. Walmsley, Phys. Rev. A **66**, 013811 (2002).

[46] A. N. Berkovsky, S. A. Kozlov, and Y. A. Shpolyanskiy, Phys. Rev. A **72**, 043821 (2005).

[47] E. M. Belenov and A. V. Nazarkin, JETP Lett. **51**, 288 (1990) [Pis'ma Zh. Eksp. Teor. Fiz. **51**(5), 252 (1990)].

[48] H. Leblond and F. Sanchez, Phys. Rev. A **67**, 013804 (2003).

[49] H. Leblond, S. V. Sazonov, I. V. Mel'nikov, D. Mihalache, and F. Sanchez, Phys. Rev. A **74**, 063815 (2006).

[50] H. Leblond, Phys. Rev. A **78**, 013807 (2008).

[51] H. Leblond, I. V. Mel'nikov, and D. Mihalache, Phys. Rev. A **78**, 043802 (2008).

[52] H. Leblond and D. Mihalache, Phys. Rev. A **79**, 063835 (2009).

[53] A. Sakovich and S. Sakovich, J. Phys. Soc. Jpn. **74**, 239 (2005).

[54] E. V. Kazantseva, A. I. Maimistov, and J.-G. Caputo, Phys. Rev. E **71**, 056622 (2005).

[55] M. Pietrzyk, I. Kanattŝikov, and U. Bandelow, J. Nonlinear Math. Phys. **15**, 162 (2008).

[56] N. Costanzino, V. Manukian, and C. K. R. T. Jones, SIAM J. Math. Anal. **41**, 2088 (2009).

[57] S. A. Skobelev and A. V. Kim, JETP Lett. **80**, 623 (2004).

[58] D. V. Kartashov, A. V. Kim, and S. A. Skobelev, JETP Lett. **78**, 276 (2003).

[59] A. Sakovich and S. Sakovich, J. Phys. A **39**, L361 (2006).

[60] S. A. Skobelev, D. V. Kartashov, and A. V. Kim, Phys. Rev. Lett. **99**, 203902 (2007).

[61] A. V. Kim, S. A. Skobelev, D. Anderson, T. Hansson, and M. Lisak, Phys. Rev. A **77**, 043823 (2008).

[62] S. Amiranashvili, A. G. Vladimirov, and U. Bandelow, Phys. Rev. A **77**, 063821 (2008).

[63] E. J. Parkes, Chaos Solitons Fractals **38**, 154 (2008).

[64] M. J. Potasek, J. Appl. Phys. **65**, 941 (1989).

[65] K. Porsezian and K. Nakkeeran, Phys. Rev. Lett. **76**, 3955 (1996).

[66] K. Porsezian, J. Mod. Opt. **44**, 387 (1997).

[67] M. Gedalin, T. C. Scott, and Y. B. Band, Phys. Rev. Lett. **78**, 448 (1997).

[68] V. N. Serkin and A. Hasegawa, Phys. Rev. Lett. **85**, 4502 (2000).

[69] E. M. Gromov and V. I. Talanov, Chaos **10**, 551 (2000).

[70] V. I. Kruglov, A. C. Peacock, and J. D. Harvey, Phys. Rev. E **71**, 056619 (2005).

[71] V. N. Serkin, A. Hasegawa, and T. L. Belyaeva, Phys. Rev. Lett. **98**, 074102 (2007).

[72] S. Zhang and L. Yi, Phys. Rev. E **78**, 026602 (2008).

[73] W.-P. Zhong, R.-H. Xie, M. Belić, N. Petrović, and G. Chen, Phys. Rev. A **78**, 023821 (2008).

[74] M. Belić, N. Petrović, W.-P. Zhong, R.-H. Xie, and G. Chen, Phys. Rev. Lett. **101**, 123904 (2008).

[75] L. L. Tatarinova and M. E. Garcia, Phys. Rev. A **78**, 021806 (2008).

[76] M. J. Ablowitz and T. P. Horikis, Eur. Phys. J. Special Topics **173**, 147 (2009).

[77] A. V. Husakou and J. Herrmann, Phys. Rev. Lett. **87**, 203901 (2001).

[78] M. Kolesik, J. V. Moloney, and M. Mlejnek, Phys. Rev. Lett. **89**, 283902 (2002).

[79] M. Kolesik and J. V. Moloney, Phys. Rev. E **70**, 036604 (2004).

[80] A. Ferrando, M. Zacarés, P. Fernández, P. Fernández de Córdoba, D. Binosi, and Á. Montero, Phys. Rev. E **71**, 016601 (2005).

[81] P. Kinsler, S. B. P. Radnor, and G. H. C. New, Phys. Rev. A **72**, 063807 (2005).

[82] V. I. Arnold, *Mathematical Methods of Classical Mechanics*, 2nd ed. (Springer, Berlin, 1989).

[83] G. Webb, M. P. Sorensen, M. Brio, A. R. Zakharian, and J. V. Moloney, Physica D **191**, 49 (2004).

[84] V. E. Zakharov, V. S. L'vov, and G. Falkovich, *Kolmogorov Spectra of Turbulence 1. Wave Turbulence* (Springer, Berlin, 1992).

[85] V. E. Zakharov, S. L. Musher, and A. M. Rubenchik, Phys. Rep. **129**, 285 (1985).

[86] V. E. Zakharov and E. A. Kuznetsov, Usp. Fiz. Nauk **40**, 1087 (1997).

[87] L. D. Landau, E. M. Lifshitz, and L. P. Pitaevskii, *Electrodynamics of Continuous Media*, 2nd ed. (Elsevier, New York, 1984).

[88] V. E. Zakharov and E. A. Kuznetsov, JETP **86**, 1035 (1998).

[89] C. Canuto, M. Y. Hussaini, A. Quarteroni, and T. A. Zang, *Spectral Methods: Fundamentals in Single Domains*, 3rd ed. (Springer, Berlin, 2006).

[90] E. Hairer, S. P. Nørsett, and G. Wanner, *Solving Ordinary Differential Equations I: Nonstiff Problems*, 2nd ed. (Springer, Berlin, 2000).

[91] I. Cristiani, R. Tediosi, L. Tartara, and V. Degiorgio, Opt. Express **12**, 124 (2004).

[92] J. K. Ranka, R. S. Windeler, and A. J. Stentz, Opt. Lett. **25**, 25 (2000).